

N70 33261
CR- 109770

Final Report
on a
50-60 GHz Latching Phase Shifter

Contract NAS 12-2159

May 28, 1970

CASE FILE
COPY

Prepared for:

National Aeronautics and Space Administration
Electronics Research Center
55 Broadway
Cambridge, Massachusetts 02142

By:

Westinghouse Electric Corporation
Defense and Space Center
Friendship International Airport
Post Office Box 746
Baltimore, Maryland 21203

MASTER

Final Report
on a
50-60 GHz Latching Phase Shifter

Contract NAS 12-2159

May 28, 1970

Prepared for:

National Aeronautics and Space Administration
Electronics Research Center
55 Broadway
Cambridge, Massachusetts 02142

By:

Westinghouse Electric Corporation
Defense and Space Center
Friendship International Airport
Post Office Box 746
Baltimore, Maryland 21203



TABLE OF CONTENTS

1. INTRODUCTION	1
2. TECHNICAL DISCUSSION	3
2.1 Principles of Operation	3
2.2 Material Considerations	3
2.3 Preliminary Analysis and Calculations	8
2.4 Device Fabrication Technology	11
2.4.1 Waveguide fabrication	12
2.4.2 Ferrite stack fabrication	17
2.5 Test Fixture Experimental Results	21
3. DISCUSSION OF FINAL PHASE SHIFTER	31
4. OPERATING INSTRUCTIONS	35
5. CONCLUSIONS AND RECOMMENDATIONS	39
6. NEW TECHNOLOGY APPENDIX	41



1.0 INTRODUCTION

The objectives of this program were to design and build a four bit, 360° , digital latching ferrite phase shifter with the following properties in the frequency bands 50-52 GHz and 58-60 GHz: VSWR as low as possible and insertion loss less than 1 dB. These objectives were to be met by trying alternative approaches, chief among which were (1) fabricating the active ferrite portion of the device from toroidal segments and placing the assembled toroidal stack in a machined waveguide housing, and (2) electroforming a waveguide structure about either a conventionally machined ferrite toroid stack or a twin slab microwave ferrite structure with the magnetic path completed external to the waveguide. The objectives and alternative approaches were thought to be challenging but reasonable based upon parameter projections from previous Westinghouse phase shifter development programs at 35 and 75 GHz. As the program developed it became clear that time and cost restrictions prohibited a thorough investigation of electroforming techniques for both the toroidal and twin slab ferrite approaches. In fact, the work that was conducted on electroforming and twin slab techniques was entirely company funded. Because of these limitations, it was decided at the end of phase I to use the past proven technique of assembling a segmented toroidal ferrite stack into a conventionally machined waveguide housing in order to create a working device by the end of the program. The decision was made knowing that achievement of the stated objectives would be compromised but realizing that even a conventionally fabricated phase shifter would provide needed experience and developmental data in this frequency range. It is still felt strongly that with a sufficiently long and thorough program devoted to an electroformed housing enclosing a twin slab ferrite stack, it should be possible to more nearly approach the original objectives. As it is, the final four bit phase shifter has the properties given in table I.



A description of operating principles, fabrication technology and design trade-offs involved in the program is given in section 2. Information concerning the delivered phase shifter is contained in section 3, and operating instructions in section 4.

Table I
50-60 GHz Phase Shifter Specifications

VSWR [*] Insertion Loss [*] Switching Speed (μ sec.) ^{**} Switching Current (amp) Switching Energy (μ joules) Peak RF Power ⁺	50-52 GHz			58-60 GHz		
	< 2:1			< 1.5:1		
	~ 4 dB			~ 5 dB		
	< 1	1	2	< 1	1	2
	3	2.09	2.07	3	2.09	2.07
	> 4.4	4.35	4.31	> 4.4	4.35	4.31
	6.2 kW			6.2 kW		

* Complete VSWR and Insertion Loss curves are given in section 3.

** These figures are for the 180° bit.

⁺ This figure is calculated based on a measured value of 6 kilowatts for a 35 GHz phase shifter.



2.0 TECHNICAL DISCUSSION

2.1 Principles of Operation

The phase shifter is composed of a series of rectangular ferrite toroids (bits) separated by $3/4 \lambda$ dielectric inserts and bounded at each end by matching transformers. This assembly is placed along the center line of a waveguide structure. The slot in the toroid is electrically loaded with a dielectric which takes up almost the entire volume of the slot. In the small air space remaining is placed a current carrying latching wire whose ends are brought out through the waveguide side wall. This structure is shown schematically in Figure 1.

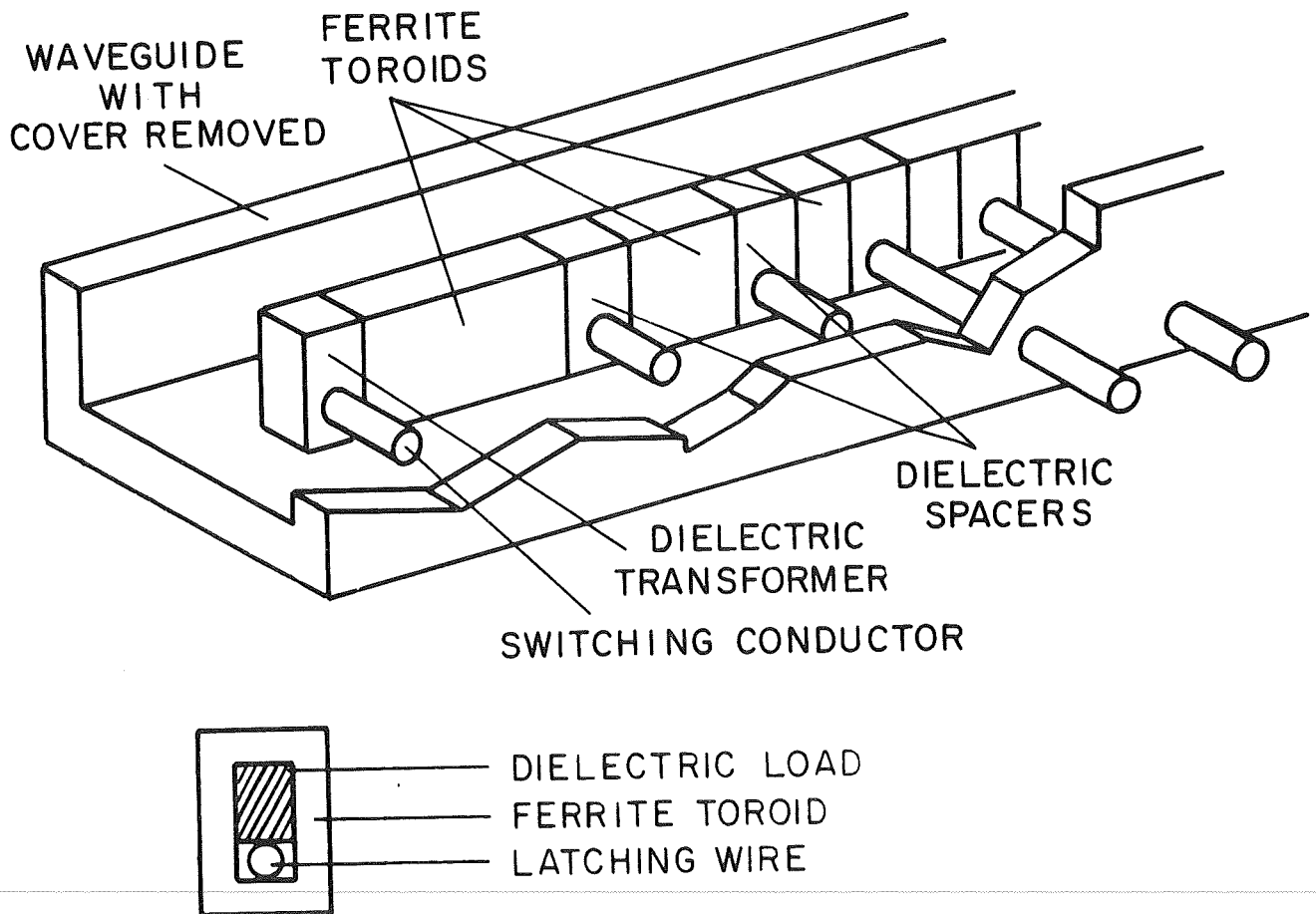
Phase shift is accomplished by switching the toroid between its two remanent flux density states. Consider the hysteresis loop for the ferrite material shown in Figure 2. When current of the appropriate polarity of magnitude sufficient to provide a field approximately 5 Hci is applied to the latching wire the ferrite saturates in one direction (say positive) and relaxes to B_r^+ . RF energy passing down the waveguide is phase shifted by an amount ϕ^+ which is proportional to μ^+ (RF permeability), which is proportional to B_r^+ . When the current in the latching wire is reversed the ferrite is forced into its B_r^- remanent state (reset). The phase shift for this condition is ϕ^- and is proportional to μ^- and B_r^- . Differential phase shift $\Delta\phi$ is given by $\phi^+ - \phi^-$.

2.2 Material Considerations

As one attempts to extend latching ferrite phase shifters into the millimeter wave region, material considerations become of the utmost importance. Ideally, for a below resonance phase shifter, the range of values for the saturation magnetization, $B_s = 4\pi M_s$, can be expressed as

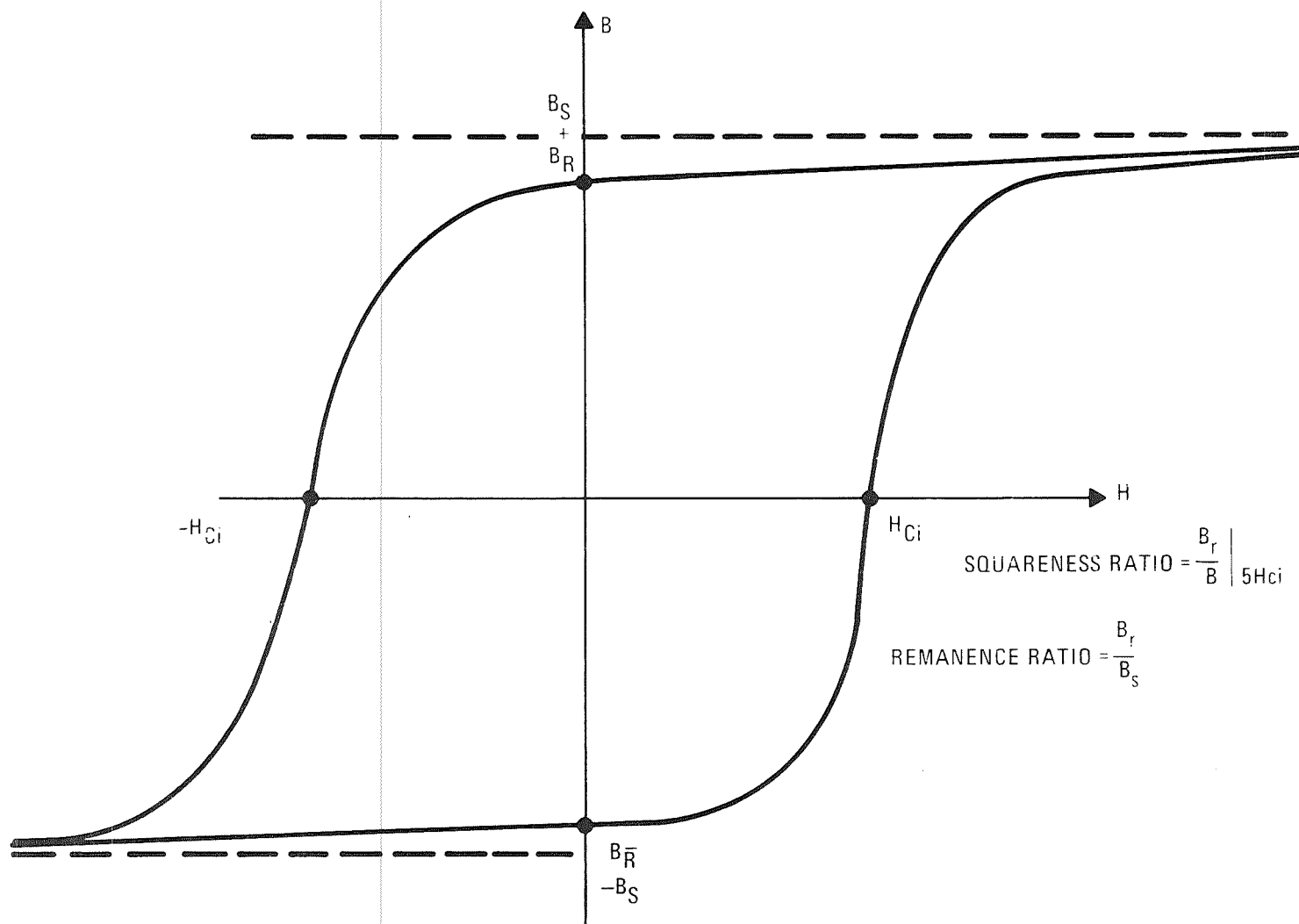
$$\left[\begin{array}{l} \text{Low Activity} \\ \text{High Peak Power} \end{array} \right] \quad 0.4 \leq \frac{\omega_m}{\omega} \leq 0.7 \quad \left[\begin{array}{l} \text{High Activity} \\ \text{Low Peak Power} \end{array} \right]$$

where



S73 49A - VA - 4-1

Figure 1. Schematic of phase shifter construction.



S70-616-VA-13

Figure 2. Hysteresis loop for a typical ferrite material. B is flux density, H is magnetic field intensity and H_{Ci} is intrinsic coercive force.



$$\omega_m = \gamma 4\pi M_s$$

$$\gamma = \text{gyromagnetic ratio} = 2.8 \text{ MHz/oersted}$$

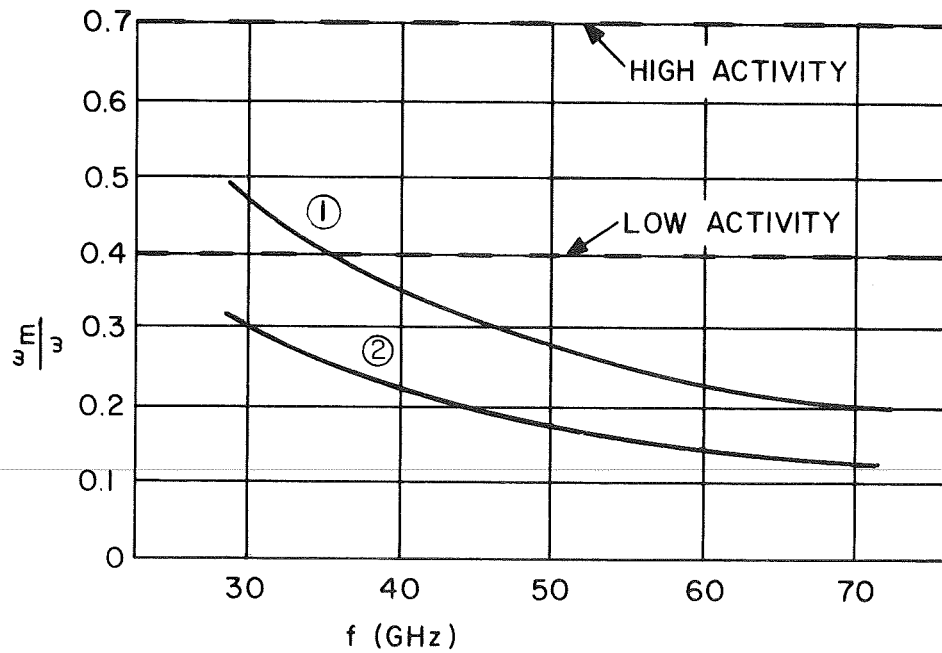
$$\omega = \text{frequency of interest}$$

For large differential phase shifts and low power requirements, the ratio $\frac{\omega_m}{\omega}$ should be made to approach the 0.7 value. For high power applications the lower bound should be approached.

At millimeter wavelengths, however, one has little choice since the largest attainable value of $4\pi M_s$ is approximately 5,000 gauss. A plot of $\frac{\omega_m}{\omega}$ for $4\pi M_s = 5,000$ gauss versus frequency is shown in figure 3. This plot clearly shows that at millimeter wavelengths one is constrained to work in the region of low activity. With this constraint (i.e., a practical maximum of 5,000 gauss for $4\pi M_s$) the next most important material considerations are squareness and remanence ratios. These quantities, which are defined in figure 2, should be as high as possible since the resultant phase shift will be proportional to B_r , the remanent magnetization.

At millimeter wavelengths, nickel zinc ferrites are a good choice since the nickel zinc ferrosphenel system yields high values of saturation magnetization due to the strong tetrahedral site preference of zinc ions. However, examination of the characteristics of a commercially available material, TT2-111*, reveals a $4\pi M_s = 5,000$ gauss but a rather poor remanence ratio of 0.42, yielding a remanent magnetization, B_r , of only 2,100 gauss. In addition, nickel zinc ferrites are magnetostrictive; i.e., their characteristics are pressure sensitive. Use of this type ferrite requires a very careful device design to provide an intimate yet low pressure contact to the top and bottom walls of the waveguide. Phase shift results were obtained using TT2-111 ferrite toroids and are cited in section 2.5; however, since an improved, non magnetostrictive

* A product of Trans-Tech. Inc., Gaithersburg, Maryland.



9274A-VA-1

Figure 3. $\frac{\omega_m}{\omega}$ for $4\pi M_s = 5,000$ gauss as a function of frequency, curve 1; curve 2, for $4\pi M_s = 3,200$ gauss.

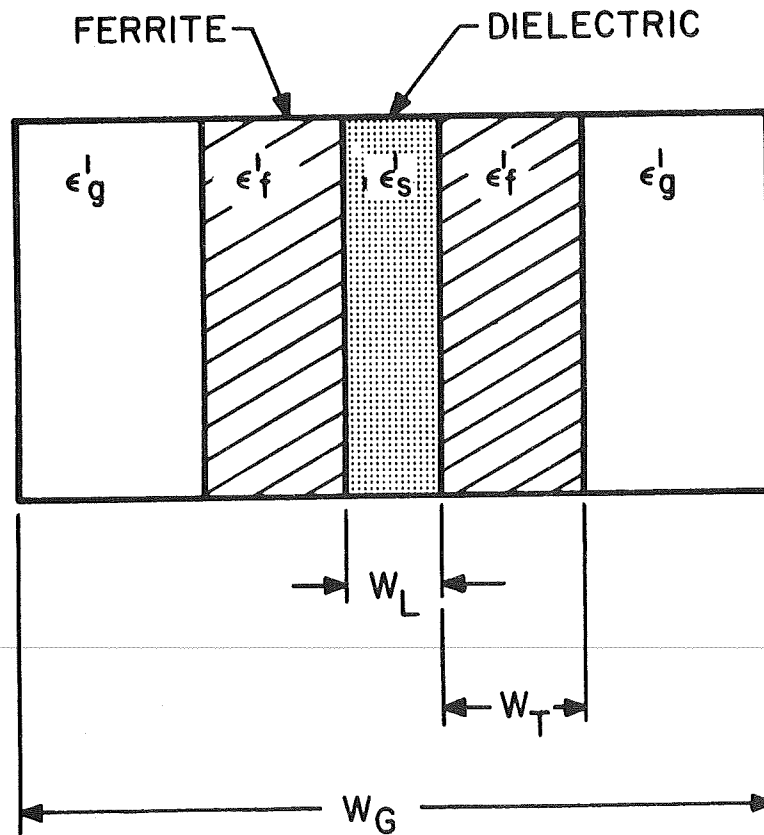


magnesium manganese ferrite was available which provided better phase shift values, it was decided to proceed with the latter material. The magnesium-manganese ferrite, commercially known as M3.2A was developed under Westinghouse auspices by Dr. Ernest Wantuch at Fairleigh Dickenson University. It has a saturation magnetization of 3200 gauss and a remanent ratio of 0.75.

2.3 Preliminary Analysis and Calculations

A computer program was developed to obtain simultaneous values of the propagation constant β , and the attenuation constant α , for the twin-slab geometry shown in figure 4. The twin slab model, while not having toroidal characteristics, is a good approximation to a toroidal geometry and is amenable to computer calculation. Phase shift magnitude and dispersion were found to depend upon a variety of parameters. The chief influencing parameters for a given magnetic material are the dielectric constant of the slab, or in the toroidal case, the slot, the thickness of the ferrite members with respect to the dielectric slab thickness, and the overall thickness of the ferrite-dielectric sandwich with respect to the waveguide width. For facility in electrical matching it was decided to use a dielectric load of ϵ'_s as close as possible to that of the ferrite. Initial calculations showed that using loads of dielectric constant values in the 30 to 50 range would permit very high phase shift to be obtained. However, good low loss high dielectric constant material was not commercially available. Using high dielectric constant material was also found to increase the tendency of the device to propagate higher order modes.

Given a ferrite $\epsilon'_f = 14$ and a load $\epsilon'_s = 13$ a series of dispersion curves was calculated, several of which appear in figure 5 with ferrite width and dielectric load width as parameters. Curve number 1 on this figure predicted a sufficiently high differential phase shift consistent with reasonably uniform



9274A-VA-3-1

Figure 4 - Geometry Used for Computer Analysis, ϵ'_g , ϵ'_f , ϵ'_s are Dielectric Constants of Side Members, Ferrite, and Slot Load, Respectively; W_G , W_T , W_s are Widths of Waveguide, Toroid Limb and Slot.

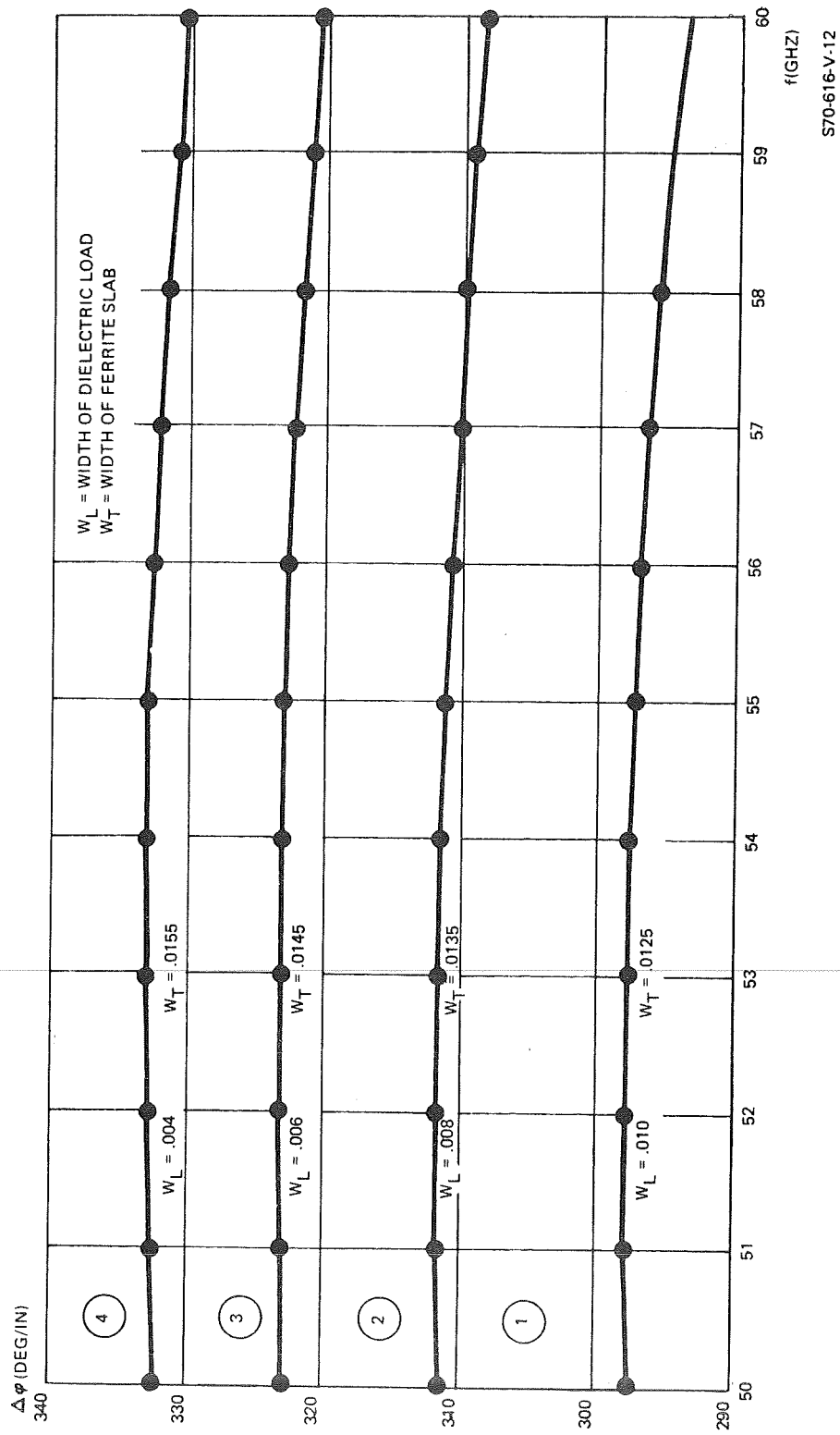


Figure 5 - Computer Calculated Phase Shifter Dispersion Curves with Slot Load Width and Ferrite Slab Width as Parameters.



dispersion and practically realizable dimensions. Calculated insertion loss values were on the order of 0.8 dB/in. based upon assuming a loss target of 0.001 for the ferrite material. This value is typical for the M3.2A ferrite used at X-band. The actual value in the 50-60 GHz range is probably considerably higher but since no measurements of loss tangent had actually been made, the X-band value was used in the calculations.

It was decided to design the phase shifter to the parameters specified by curve 1. The actual phase shift was not expected to equal that predicted because of (1) the non contribution to total phase shift by a portion of the horizontal and vertical members of the toroid, and (2) the decrease in effective dielectric constant due to tiny air spaces in the toroid slot. Maximum phase shift is obtained only where the latching and RF magnetic fields are perpendicular. In the toroid the curvature of the latching field near the corners results in small phase shift in these regions.

2.4 Device Fabrication Technology

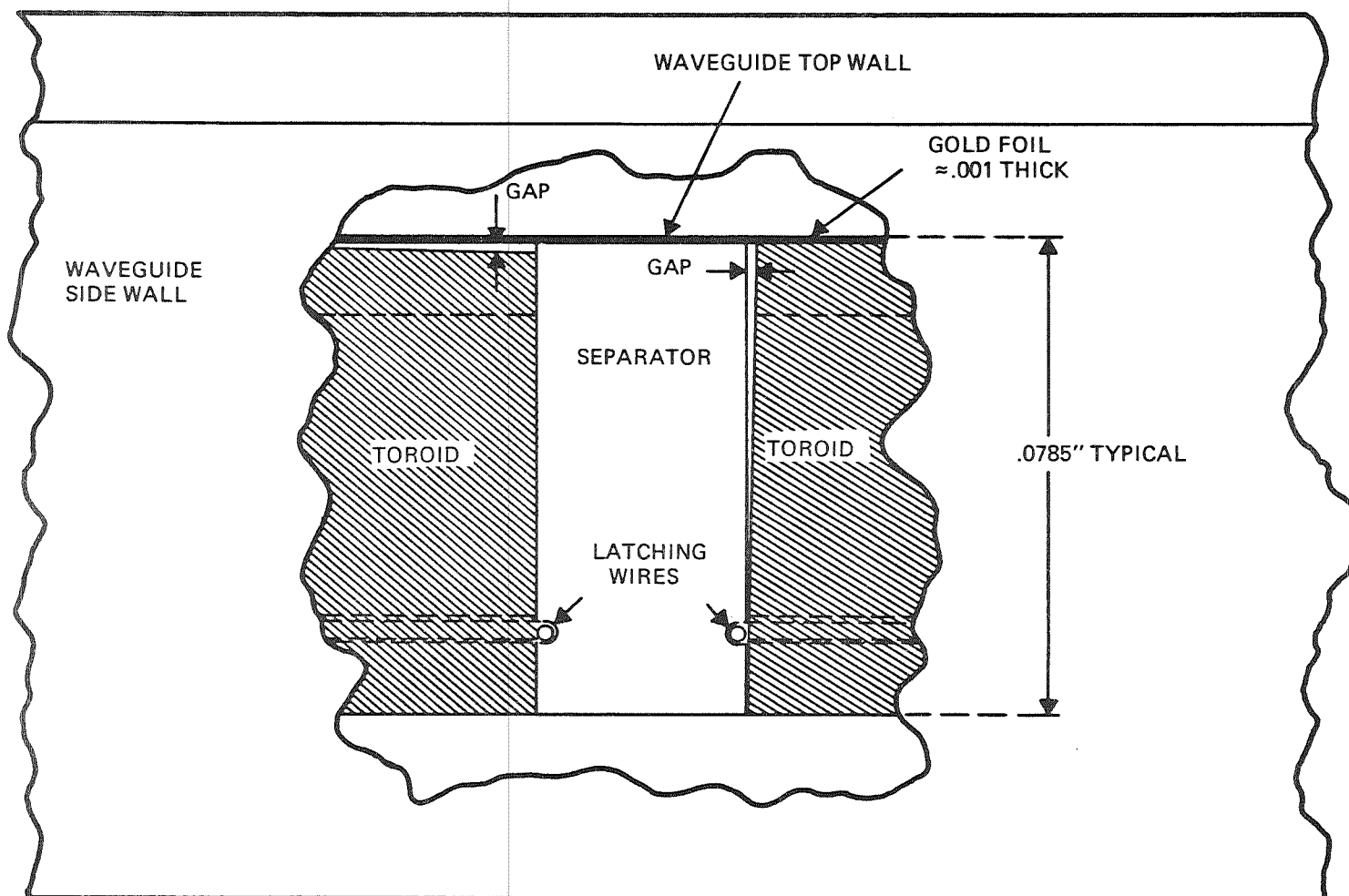
Operationally, the program for building the phase shifter logically subdivided into two major tasks. These were (1) constructing the waveguide housing from either a machined fixture or by means of electroforming techniques, and (2) fabricating the ferrite stack from either a series of separately machined toroids or a series of ferrite-dielectric twin slab sandwiches. The ferrite fabrication subtask depended in several ways upon the waveguide construction methods; thus it was initially decided to make a machined waveguide test fixture housing, perform measurements using conventionally fabricated toroids in this fixture, and simultaneously mount a parallel development effort in electroforming techniques and twin slab fabrication. In this way it appeared to be possible to achieve basic information in a conventional fixture, meanwhile developing an electroforming technique which might be used in a final device. A more detailed description of the subtasks is given in the following sections.



2.4.1 Waveguide Fabrication

2.4.1.1 Machined Waveguide

It was observed from the many experiments performed in a machined waveguide test fixture, that no real advantage is offered by this configuration, except that of relatively rapid fabrication. The $1\frac{1}{2}$ " long test fixture was machined from two pieces of brass, one containing the bottom and side walls of standard RG-98/U waveguide and the other forming the top wall. The empty fixture loss after gold plating was .25 dB. A shallow slot of the same width as the toroids was milled down the center of the lower waveguide wall for the purpose of locating the toroids and matching transformers. The toroids, separators and transformers were placed in the lower half of the guide, malleable gold foil of toroid width was placed along the top and bottom of the toroid stack, and the two waveguide halves were then bolted together. The procedure sounds quite simple but in fact, is not! Good phase shift and low VSWR and insertion loss performance strongly depend upon the intimate and uniform contact of the top and bottom waveguide walls with the toroid stack and intimate toroid to toroid contact. It was attempted to provide this contact by insisting on extremely precise dimensional tolerances for all components, by applying great care in cleaning and assembly, and by utilizing malleable gold foil as mentioned. However, because of the small size of the components at these frequencies, even minute departures from specified dimension were strongly reflected in poor insertion loss and VSWR performance. An indication of this situation is shown schematically in figure 6. The figure is a view through the waveguide side wall and shows an enlarged representation of the junction of two toroids and one separator of the many composing the ferrite stack. It is clear that even very small dimensional deviations create air spaces where none should be. It was found that improved performance was obtained, up to a point, as the pressure on the ferrite stack was increased by tightening the waveguide housing bolts. However, this frequently resulted



S70-616-V-5

Figure 6 - Schematic Looking Through the Side of the Phase Shifter at the Junction of Two Toroids and a Separator. Two types of Gap Discontinuities are Shown.



in shattering the brittle toroids and necessitated complete reassembly. It was also an expensive process, since each toroid required approximately 4 man-hours to fabricate.

Other deficiencies in the machined waveguide housing were the presence of discontinuous junctions between the top and side walls and the difficulty in achieving an extremely smooth machined guidewall surface. The smooth wall surface in the test fixture was obtained by a combination of obtaining the best possible machine finish, hand polishing, and then gold plating.

The machined waveguide housing used in the final phase shifter consists of four pieces, a top and bottom wall and two side wall members. These also were machined to a smooth finish, hard polished, and gold plated. However, the four discontinuities at the wall junctions increased the empty fixture loss to 2 dB compared to a value of 0.6 dB projected from the measured value on the $1\frac{1}{2}$ " test fixture. The reasons for choosing this method of housing fabrication were: (1) During the early part of Phase II; considerable problems with toroid breakage had been experienced and it was thought desirable to experiment further with the twin ferrite slab approach in parallel with the toroid approach. (2) Insertion loss and VSWR spikes due to higher order modes had been observed and narrowing the waveguide width was considered as one approach to eliminating at least one of these higher order modes (LS_{20} , see section 9.5). Both of these problems required a fixture with considerable flexibility. By making the fixture in four pieces (top, bottom, and two side walls) it was possible to vary the width by a relatively simple machining of different sets of side walls; similarly different sets of top and bottom walls could be interchanged for experiments with the twin ferrite slabs. However, the price of this flexibility was increased loss and as the program approached its end it was necessary to use this housing for the final shifter rather than incur the expense and time delay (two to three weeks) involved in building a new one.



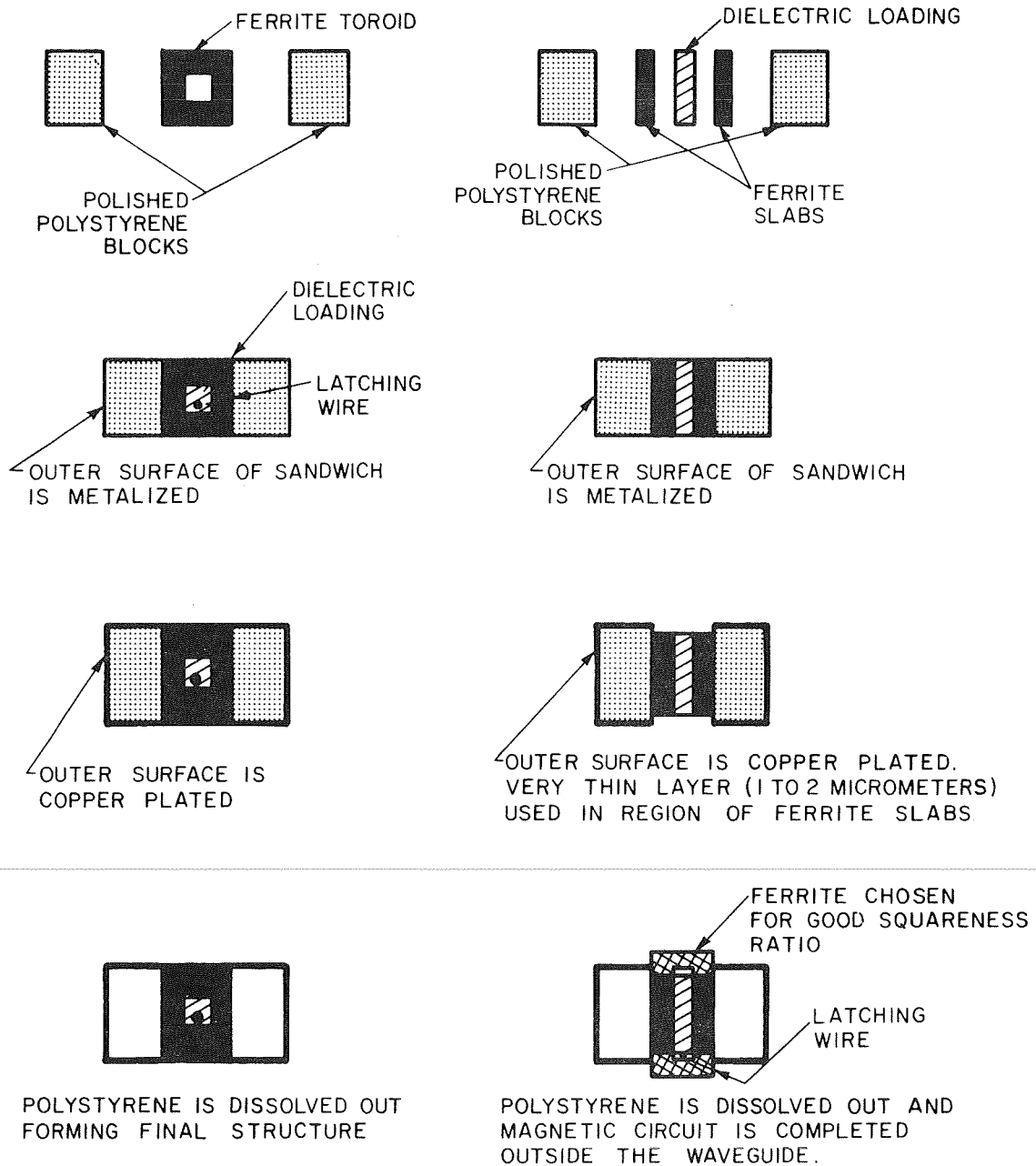
2.4.1.2 Electroformed Waveguide

The electroforming process consists basically of plating a metal such as copper (or nickel if a magnetic material is required) onto a removable (stainless steel) or dissolvable (polystyrene) mandrel of the desired shape. Polished stainless steel mandrels are useful where the shape of the final structure allows easy removal. An example of this would be a waveguide horn antenna. Polystyrene mandrels are needed where the shape is such that the mandrel must be dissolved out of the final structure. An example of this might be a millimeter wave multi-hole directional coupler. Polystyrene mandrels are also convenient where large numbers of pieces are required, since they can be formed by injection molding at a very low cost with excellent reproducibility.

Electroforming techniques are ideally suited for fabricating the 50-60 GHz latching phase shifter housing. The advantages of electroforming for this application are (1) smooth interior finish leading to lower losses, (2) elimination of gaps and discontinuities in the housing, and (3) intimate contact between the housing and the ferrite structure (toroid or twin slab) is automatically ensured. Figure 7(a) illustrates the electroforming fabrication procedure using conventional ferrite toroids. Figure 7(b) illustrates the procedure using ferrite slabs with the magnetic circuit completed outside the waveguide. The relative merits of the two geometries shown in Figure 7 are discussed in detail in the next section. With regard to the electroforming procedure itself, the main disadvantage is the more extensive (time and cost) development required to perfect this technique. For instance with the limited time scale available during the first phase of this program, the electroforming technique study had progressed to the point of injection molding and copper plating of mandrels for straight sections of RG-98/U waveguide plus one attempt to imbed a 1 inch ferrite toroid stack ($\sim 180^\circ$) in a polystyrene mandrel. For the former experiment, waveguide tolerances of .0001" were achieved. For the latter experiment .002" deep slots one inch in



ELECTROFORMING PROCEDURES FOR 50-TO 60-GHZ FERRITE PHASE SHIFTERS



(A) USING CONVENTIONAL TOROIDS

(B) USING FERRITE SLABS

9274A-VA-9

Figure 7. Left: Construction details using toroids;
Right: Electroformed housing about a twin slab ferrite stack.



length and .030" wide were milled in the top and bottom walls of the steel mold to capture the ferrite toroids (plus two $\lambda/4$ transformers). The ferrite stack plus latching wire was then placed in the mold followed by the polystyrene injection. The experiment was successful in that the latching wires remained intact (there was some fear that they might be ripped out by the inflowing polystyrene which was under several thousand pounds/sq. inch pressure). It was unsuccessful because every toroid was cracked. (This occurred during mold assembly prior to polystyrene injection). The latter circumstance emphasizes a major problem to be solved in any future development program; i.e., how to hold the toroids (or twin slabs) firmly in the mold without crushing them.

Summarizing, electroforming the phase shifter housing offers significant fabrication and performance advantages although much further development is required.

2.4.2 Ferrite stack Fabrication

2.4.2.1 Machined Toroids

The only advantage gained by using toroids machined from ferrite bar stock was that of a readily available fabrication technique. As in previous Westinghouse 35 and 75 GHz phase shifter programs, ferrite blanks were cut and ground from bar stock, the blanks were cut to a 0.2 in. length, and a rectangular slot was ultrasonically bored along the length of each piece. The 0.2 in. length was determined by experiment to be the maximum length which would permit the slot to be cut without sidewise excursion of the boring tool. Thus, in the final phase shifter all bits except the 22.5° were composed of a series of 0.2 inch toroidal segments butted end to end. This is not the best arrangement for preventing VSWR maxima due to the propagating and trapped higher order modes; each toroid junction acts as a potential source of multiple reflections which will be apparent in a VSWR record. Furthermore, dielectric loading cannot be uniform along the length of the toroid stack because of random geometrical



imperfections in the toroid slots and in the dielectric load slab matched to each toroid. Tiny height variations of the order of tenths of a mil from toroid to toroid created problems in securing an intimate contact to the top and bottom guide walls along the length of the stack. The use of malleable gold foil between the upper and lower toroid surfaces and top and bottom guide walls helped to ameliorate this problem, but it was never possible to maintain perfect wall contact with all the toroids simultaneously. This problem is indicated in the schematic of figure 6 where a small gap is shown between the top surface of a toroid and the gold foil. Contact could be improved by tightening the waveguide housing screws, only, however, at risk of cracking one or several of the highest and/or weakest toroids. This latter circumstance illustrates the fundamental difficulty and source of cost in fabrication by machining: At the frequencies considered, the basic components are quite small. These components are made of ferrite and ceramic materials of low resilience. The stock materials from which the components are cut sometimes contain undetectable flaws which appear in the components as points of breakage. These several effects make the machined fabrication of separate toroids a costly and time consuming process.

The final disadvantage of the toroidal configuration as compared with a twin slab geometry is that not all of the ferrite is available for phase shift. The horizontal toroid members contain a latching magnetic field parallel to the RF field. No phase shift occurs in these members.

2.4.2.2 Ferrite Twin Slab Technology

The inherent disadvantages of using machined toroids were noted early in the program and attempts at twin slab fabrication were initiated. Since funds were limited, these experiments were carried out on a parallel program funded by Westinghouse. First, an experiment to determine the effect of completing the magnetic path of a twin slab configuration with a similar magnetic material



was performed. In this experiment, a toroid of M3.2A material with limb length of 0.6 inch and cross sectional areas of $.04 \text{ inch}^2$ was cut into two pieces as shown in figure 8(a). The mating interfaces of both pieces were precisely lapped, then vapor deposited with 0.1μ of chromium and 1.9μ of nickel. The pieces were clamped together to re-form a toroid and the hysteresis loop was measured and compared with that of a similar uncut toroid. The two hysteresis loops were not distinguishable after lapping and vacuum deposition methods were perfected. Figure 8(b) shows the hysteresis loop for the uncut toroid displayed as an oscilloscope trace. Figure 8(c) shows the loop for the re-formed toroid displayed with the oscilloscope gain controls left unchanged. These results were quite remarkable. However, when the same experiment was performed with cut toroids of the same size as those used in the phase shifter, poor results were obtained. This is so because mating surface imperfections in the much smaller phase shifter toroid comprise a much greater percentage of the surface area, with the net result being the creation of a high reluctance path. Here again, rather than spend too much time and money on an advanced development program to reduce the effect of small imperfections, it was decided to proceed with the conventional approach.

A small parallel program of twin slab fabrication was carried out during phase II of this contract in which problems of ferrite-dielectric bonding were investigated. Lapping techniques were developed which resulted in the achievement of one inch long ferrite-dielectric sandwiches which varied less than 0.0001 " in height along its length. A machined waveguide housing with nickel top and bottom walls was built for RF testing of the twin slabs, but the program ended before any testing was accomplished. Conclusions derived from the

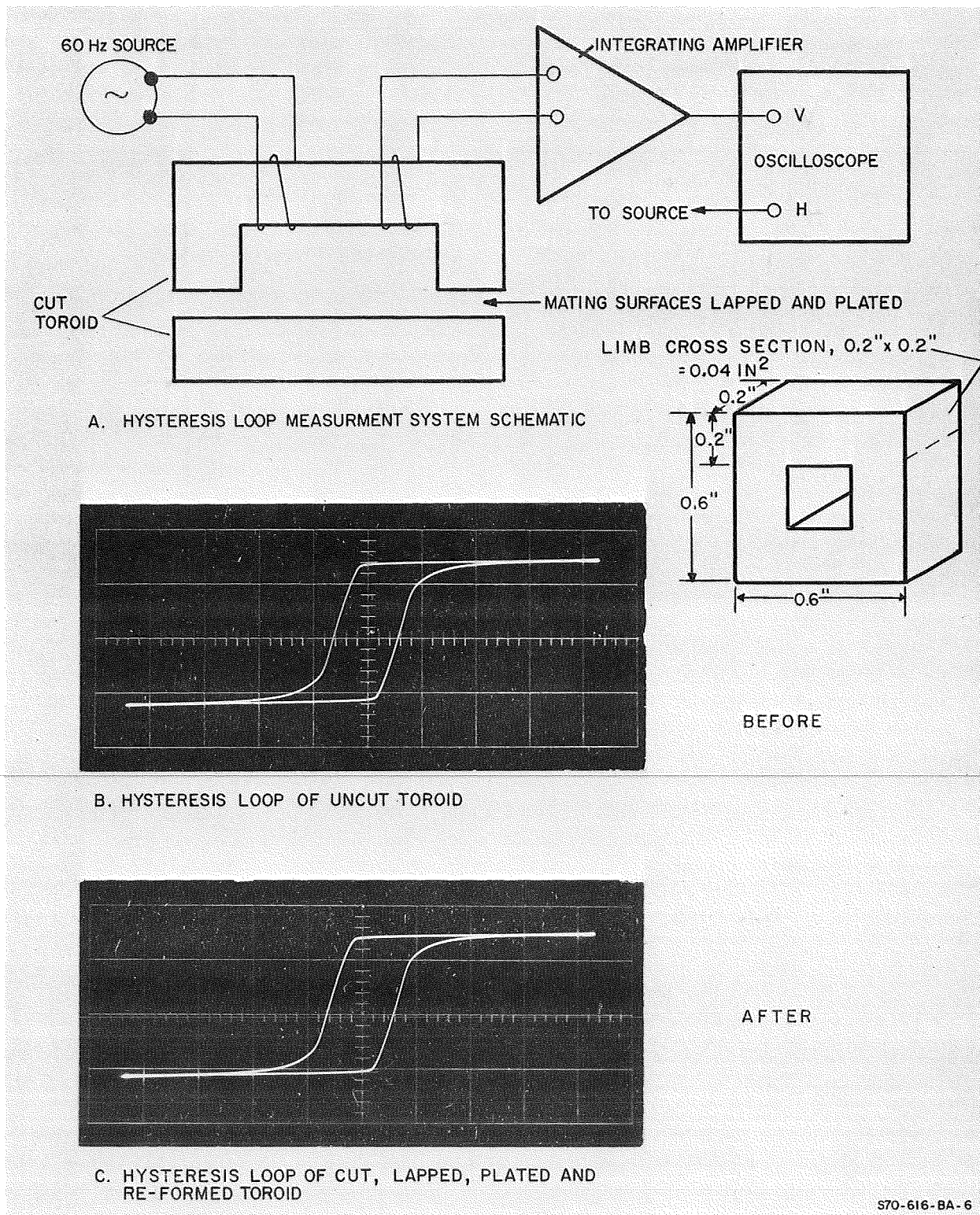


Figure 8. Magnetic path completion experimental results.

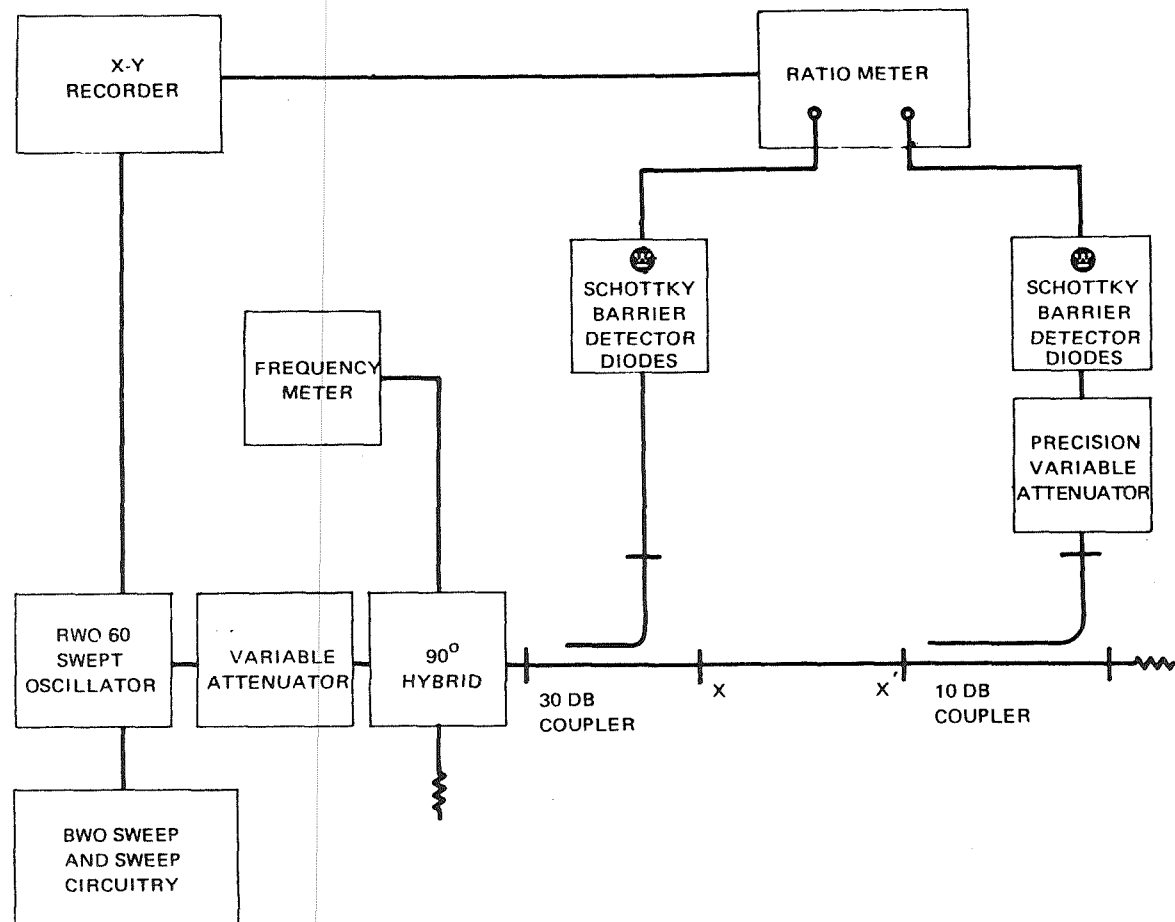


present level of twin slab fabrication are: (1) The approach shows promise in that it permits the construction of longer ferrite stack elements. Thus it is not necessary to construct the phase shifter bits of a multitude of 0.2 in. long segments, as with toroids. (2) It is easier and potentially less expensive to fabricate thin slabs of ferrite and dielectric material than it is to make toroids. (3) It is possible to form an intimate bond between the two ferrite slabs and the dielectric center slab. This is not possible with slot loaded toroids. The one remaining question--can the magnetic path be completed with negligible loss in remnant magnetization?--requires a longer and more thorough investigation although results with larger toroids seem to indicate that it can indeed be accomplished.

2.5 Test Fixture Experimental Results

As the program developed, a continuing series of VSWR, insertion loss and differential phase shift measurements were performed using a machined waveguide test fixture. The test fixture consisted of a 1.5 inch long two piece waveguide housing similar to that shown schematically in figure 6. The top lid of the housing was easily removable to permit insertion and removal of ferrite stack components, matching transformers, higher order mode suppressors, etc.

VSWR and insertion loss measurements were performed in the reflectometer arrangement shown in figure 9. Differential phase shift measurements were made in the phase bridge illustrated in figure 10. VSWR and insertion loss measurements were facilitated by using a variable frequency source, a Siemens BWO, model RW060, capable of being swept between 40 and 60 GHz. A continuing series of measurements were made as the program progressed which contributed to a voluminous and well documented data record. A small portion of this record will appear in the following figures to illustrate salient techniques and results. Early in the program it was determined that M3.2A material gave a better phase shift per inch figure than TT2-111 ferrite, (160°/in. vs 110°/in). This result, in combination



S70-616-V-1

Figure 9. 50 to 60 GHz reflectometer measurement system shown for insertion loss test. After calibrating system, guide section XX' is replaced with phase shifter.

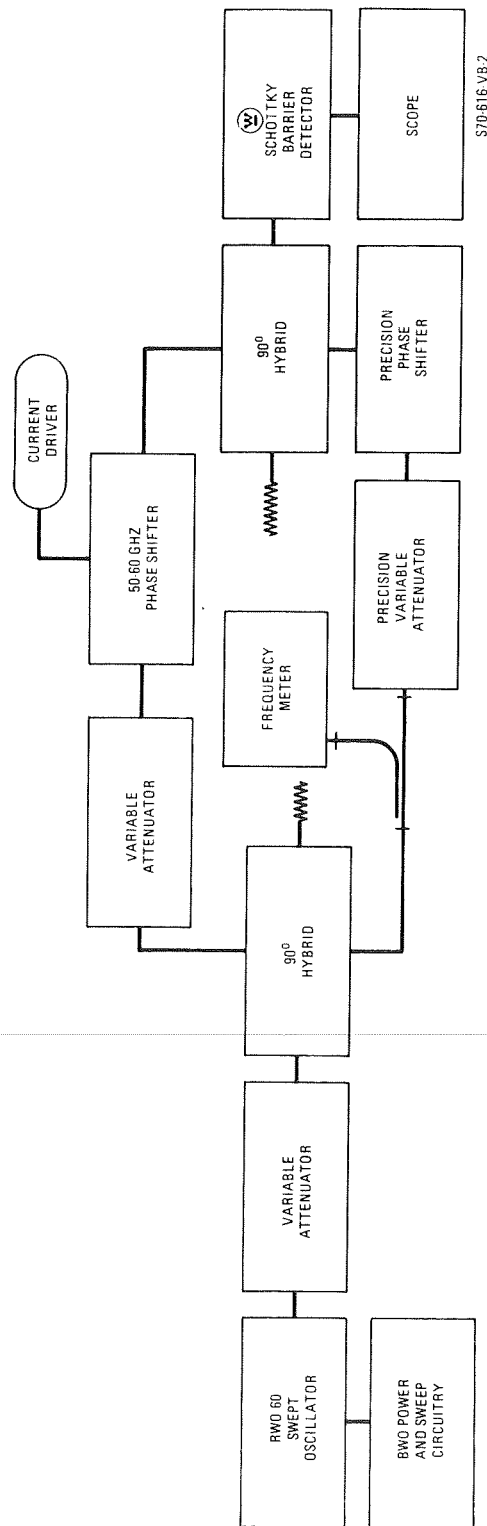


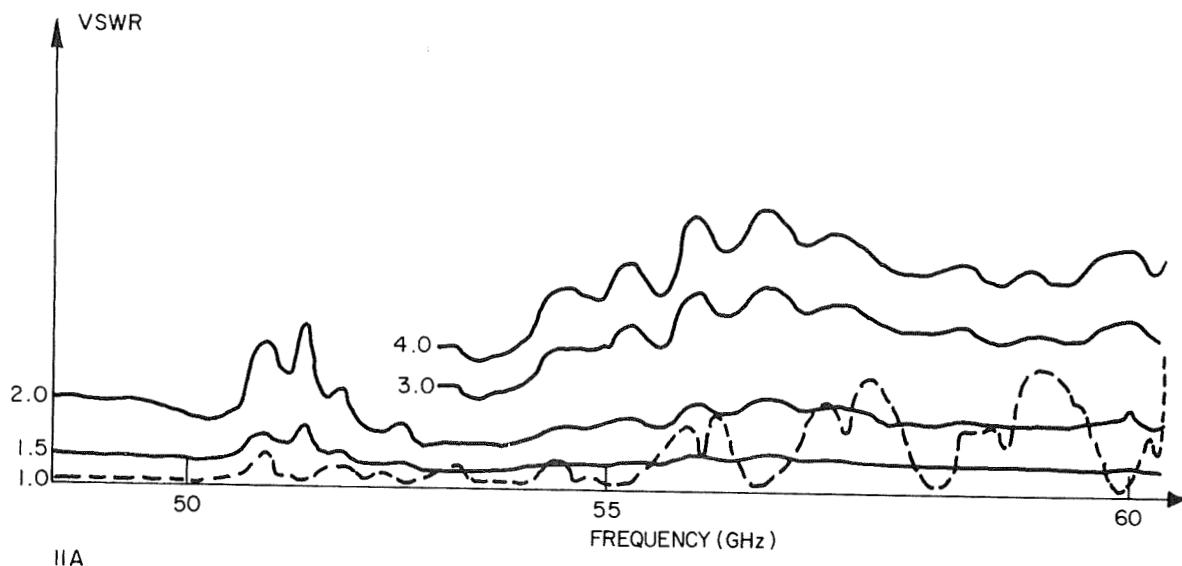
Figure 10. 50-60 GHz phase bridge arrangement.



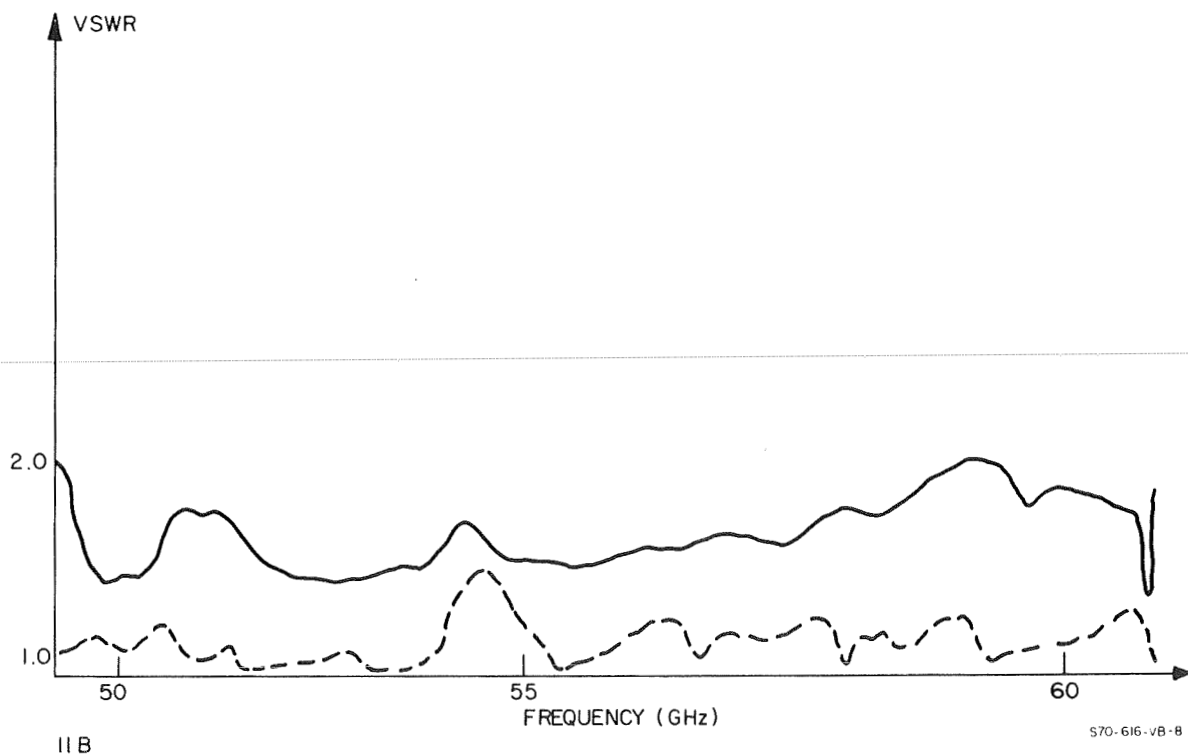
with the non magnetostrictive quality of M3.2A dictated its use in all further tests and in the final device.

After the basic ferrite stack dimensions and dielectric constant had been determined (0.35 in total toroid width, .010 in. slot width, $\epsilon'_s \approx 13$) a series of matching experiments was carried out. Several types of transformers were tried, single and double section quarter wavelength, and tapered sections. Best results were obtained with the two section quarter wavelength type which were also relatively easy to fabricate. Experiments were tried using solid dielectric slabs of the same dimensions as a one inch long toroid stack. Dielectric constants were chosen to be close to typical ferrite values (12 to 14). The slab dielectric was used to simulate a ferrite stack with no discontinuities, thus in this configuration the only internal discontinuities influencing VSWR were those between the slab and matching transformers. Figure 11 illustrates the better match obtained with a two section quarter wave matching transformer. Figure 11a shows a VSWR record from 50 to 60 GHz using a single quarter wave section of boron nitride ($\epsilon' = 4.3$) with a dielectric slab of $\epsilon'_s = 12$. VSWR maxima greater than 2:1 appear near the upper part of the band, due to end-to-end reflections. The presence of trapped higher order modes is also indicated by the VSWR spikes in the upper half of the band. By comparison, figure 11b shows VSWR for a one inch ferrite stack composed of five 0.2" long toroids matched with a two section transformer made of teflon and styrcast ($\epsilon' = 2.1$ and 8, respectively). Even considering the VSWR contribution of the toroid junctions, the overall VSWR is less than 2:1 at its highest and less than 1.5:1 over most of the curve.

The three curves of figure 12 were recorded for a five toroid ferrite stack matched as mentioned in the preceding paragraph. They illustrate a variety of effects: (1) Relatively low overall VSWR and insertion loss performance due

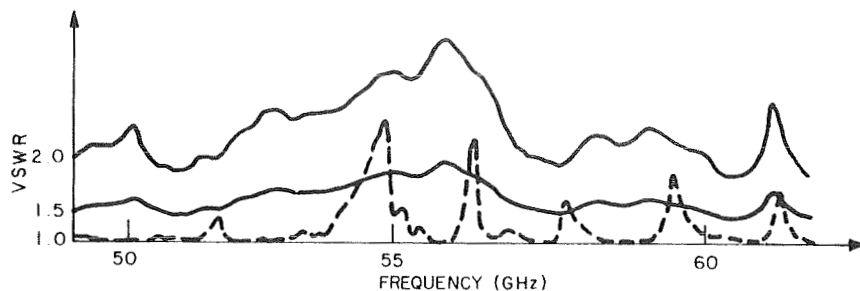


(a) Solid curve, calibration; dotted curve, measurement. Matching with single section, quarter wavelength transformer.

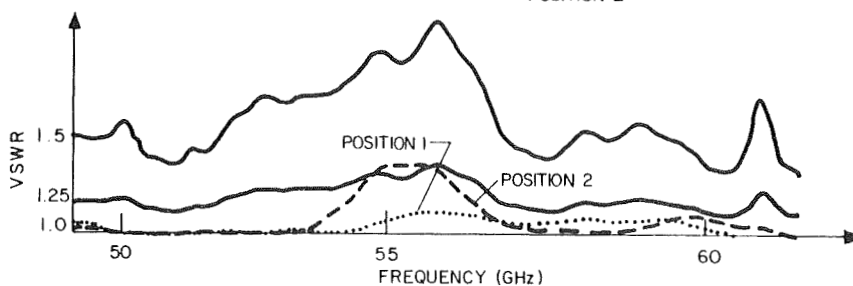
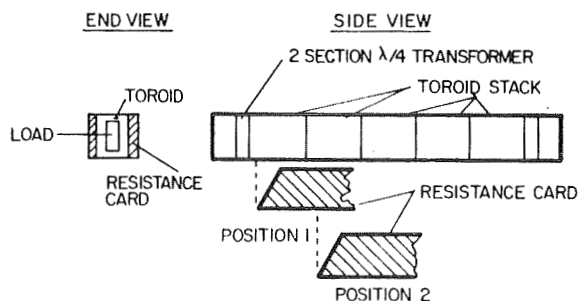


(b) Matching with double section quarter wavelength transformer. Solid, calibration; dotted, measurement.

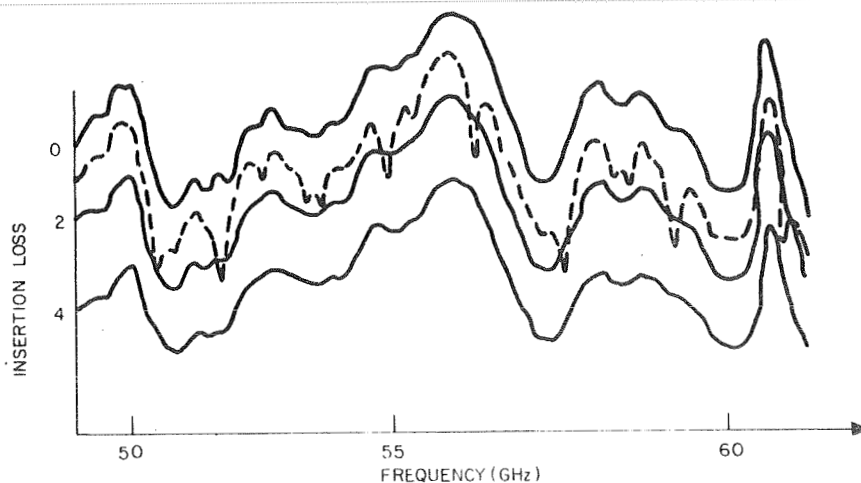
Figure 11. Impedance matching results.



(a) Overall device VSWR.



(b) VSWR using retractable resistance cards.
Insert shows resistance card configuration.



(c) Insertion loss without resistance cards.

Figure 12. Illustration of relatively good VSWR and insertion loss due to good construction; also, multiple reflection effects. Solid curves, calibration; dotted curves, measurement. All curves are for 180° bit.



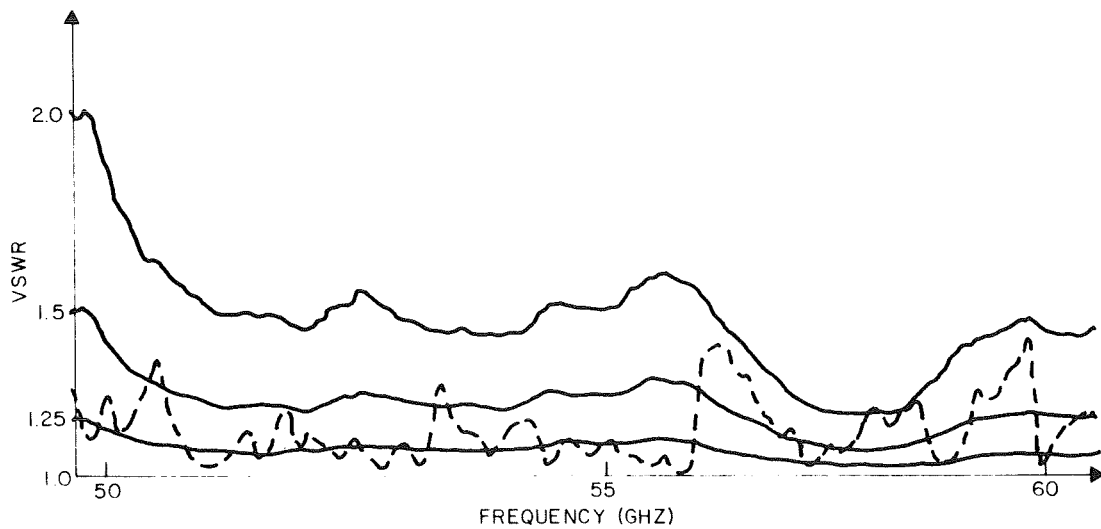
to good assembly technique. This behavior was in direct proportion to the amount of painstaking care exerted to insure waveguide smoothness, precisely matched toroid dimensions and the correct thickness of gold foil between toroids and waveguide. (2) The good impedance match provided by a two section transformer and contribution to total VSWR by the toroidal discontinuities. This is shown in figures 12a and 12b. Figure 12a presents a VSWR record taken looking into one end of the phase shifter and is the overall device VSWR composed of reflection contributions from end mismatch and from toroid discontinuities. For the VSWR curve of figure 12b, tapered cards of resistively coated .005 in thick mica were positioned alongside the ferrite stack. The cards absorbed most of the RF energy propagating beyond the tapered section. By retracting the cards along the length of the segmented ferrite stack as shown in the insert, the contribution of each discontinuity to the overall VSWR was observed. Figure 12b shows the effect of positioning the cards at two locations. The curve for position 1 shows VSWR due to end reflection and to two segment discontinuities. It is below 1.25:1. At position 2, uncovering a third discontinuity, the VSWR is slightly greater than 1.25:1 at 55 GHz but is still rather low over the rest of the range. (3) The effect of higher order mode reflections. This can be seen in figures 12a and 12c as sharp corresponding peaks in both the overall VSWR and insertion loss records.

The occurrence and elimination of higher order modes in phase shifters of this configuration has been described by Tsandoulas, et. al.⁽¹⁾ Longitudinal section modes propagate in the phase shifter with the LSE_{10} mode dominant. Spurious VSWR and insertion loss peaks are caused by higher order LS modes in addition to dominant mode multiple reflections.

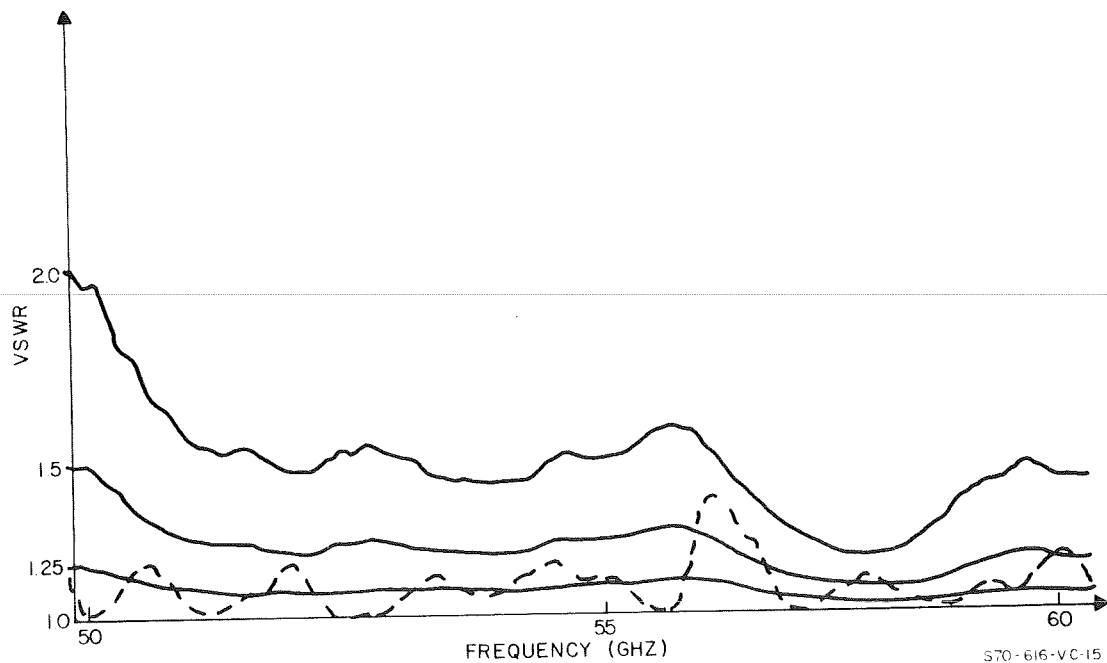
¹. Tsandoulas, G. N., Temme, D. H., and Willwerth, F. G., "Longitudinal Section Mode Analysis of Dielectrically Loaded Waveguides with Application to Phase Shifter Design," IEEE Trans. MTT, Vol. 18, No. 2, pp. 88-95, (Feb. 1970).



Mode suppression experiments involved narrowing the guide width, with only limited success. However, when thin 100 Ω /square resistance cards were inserted in the guide on both sides of the ferrite stack, significant smoothing of the VSWR and insertion loss resulted. The cards were aligned down the center of the guide, parallel to the H plane, and were supported by small styrofoam blocks. The results suggest that the annoying modes were most probably the $1SE_{11}$ and $1SM_{11}$ since both have their maximum E field parallel to the H plane at guide center. Figures 13a and 13b show VSWR curves before and after insertion of the mode suppressors. Most fine structure irregularity is removed even though larger scale variation persists. This variation is due to the multiple reflections set up in the dominant mode by ferrite stack discontinuities. Figure 14a and 14b show insertion loss before and after card insertion. As expected, the overall loss level is increased by a fraction of a dB but the fine structure irregularities were diminished.

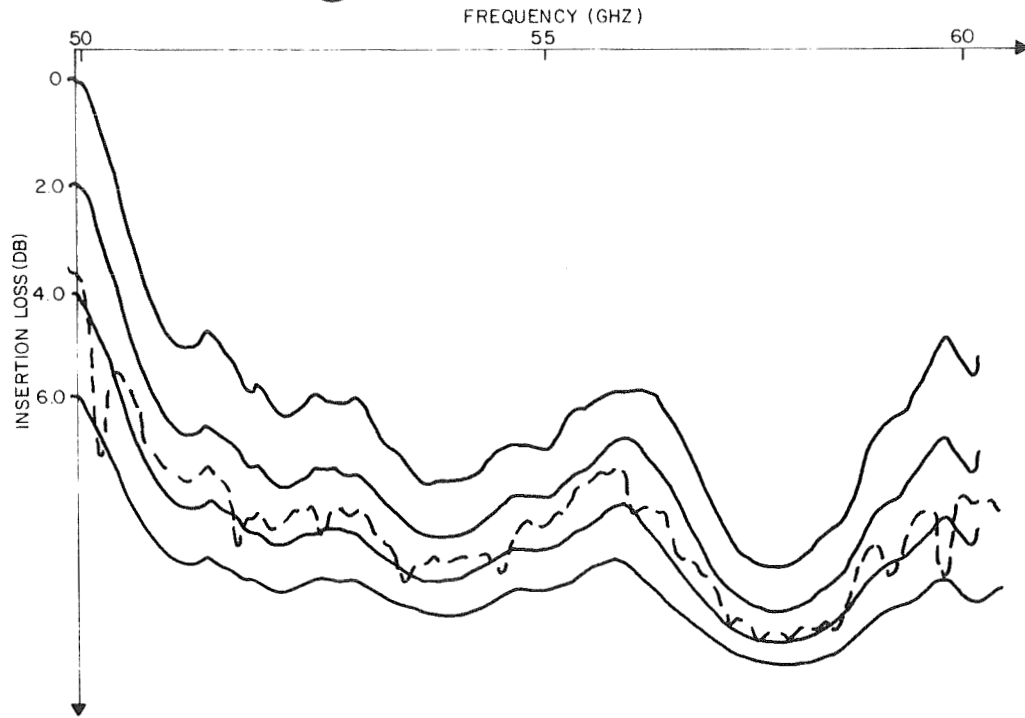


(a) Highly irregular VSWR before mode suppressor insertion.

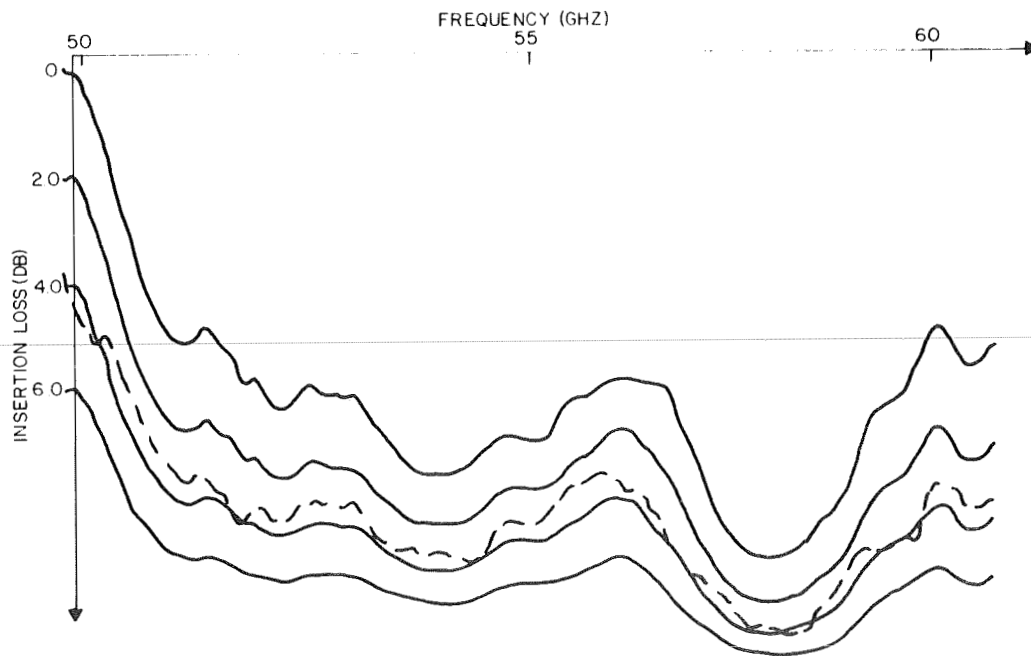


(b) Mildly irregular VSWR after mode suppressor insertion.

Figure 13. VSWR before and after mode suppression. Solid curves; calibration; dotted curves, measurement.



(a) Insertion loss before insertion of mode suppressors.



(b) Insertion loss after insertion of mode suppressors.

Figure 14. Insertion loss before and after mode suppression.
Solid curves, calibration; dotted curves, measurement.



3. DISCUSSION OF FINAL PHASE SHIFTER

As mentioned in previous sections, several circumstances influenced the decision to fabricate the phase shifter by conventional machining techniques. Success was not achieved in electroforming early enough to be of use. Twin slab bonding and lapping techniques were developed to a useful point late in the program, only after conventional fabrication was almost complete. The delivered phase shifter housing consists of a conventionally machined waveguide built up of four separate pieces bolted together. This mode of construction was decided on to permit narrowing the guide width if it were deemed necessary; it also permitted the guide height tolerance to be maintained to within 0.0003" over a four inch length by using surface ground gold plated stainless steel side pieces. It has the disadvantage of higher insertion loss due to the four discontinuous wall junctions.

A photograph of the final phase shifter with its top wall removed appears in figure 15. Toroid junctions are not visible in this figure. In the delivered device a mode suppressor is inserted into the guide on the opposite side from the latching wires. A full four bit differential phase shift curve for the final device is shown in figure 16. Insertion loss and VSWR curves are given in figure 17. The differential phase shift from 50 to 60 GHz is quite close to the 337.5° required. Insertion loss is higher than that projected from the test fixture and is due to the four wall discontinuities and mode suppressor presence. The loss averages close to 4 dB between 50 and 52 GHz and approximately 5.5 dB between 58 and 60 GHz. VSWR for these same two frequency ranges is, respectively, less than 2:1 and 1.5:1.

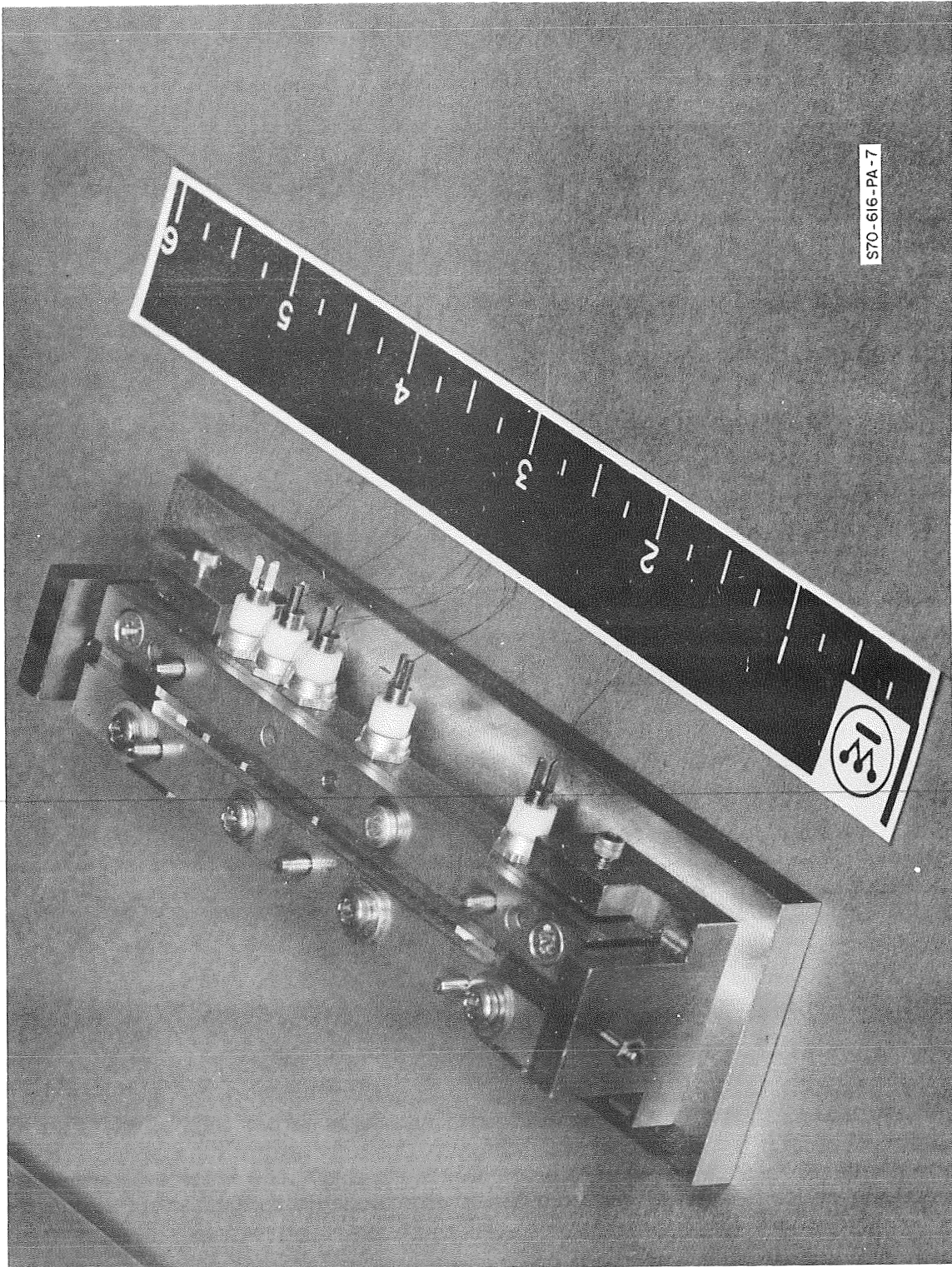


Figure 15. Delivered phase shifter with top wall removed.

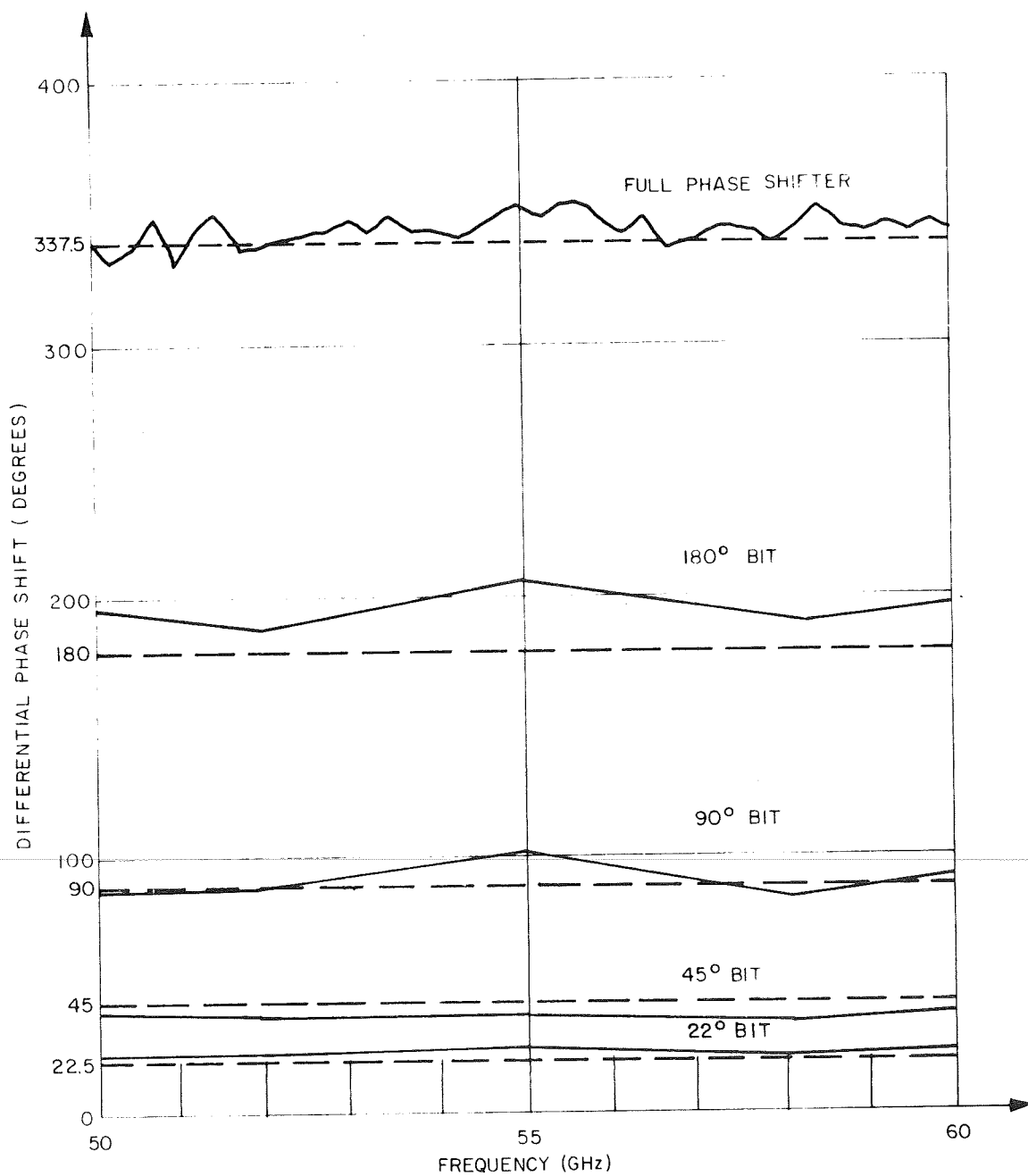
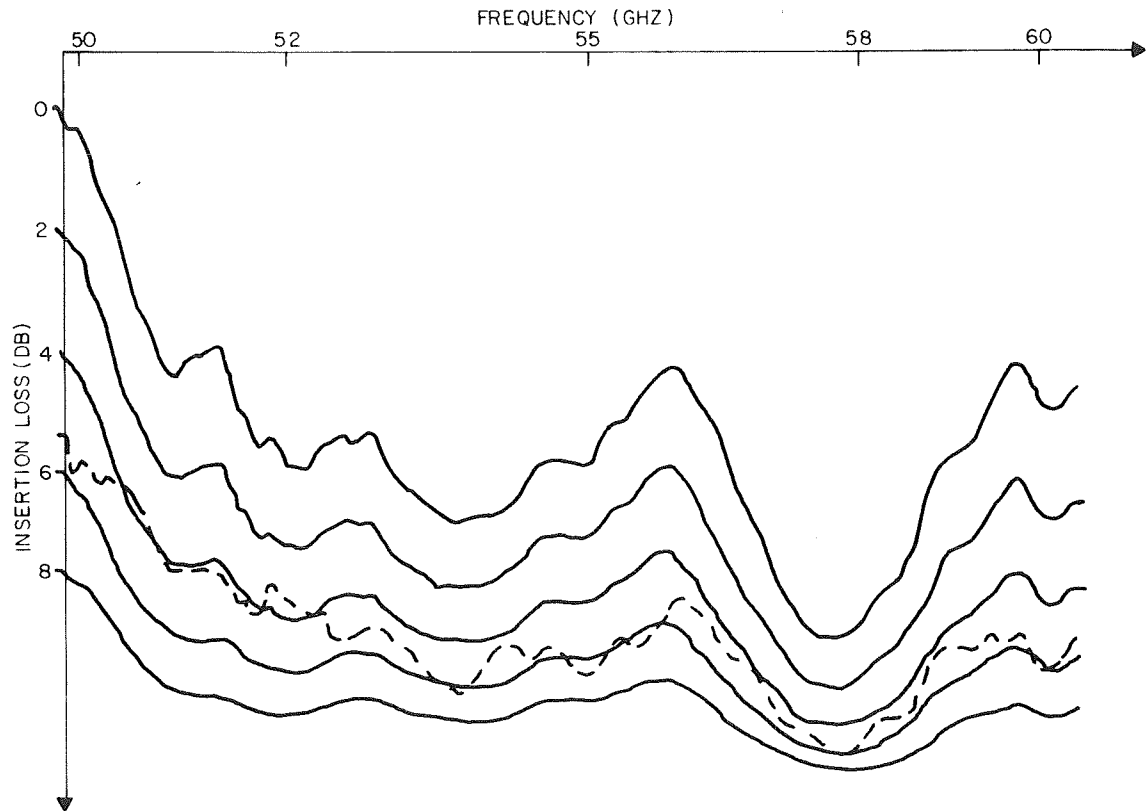
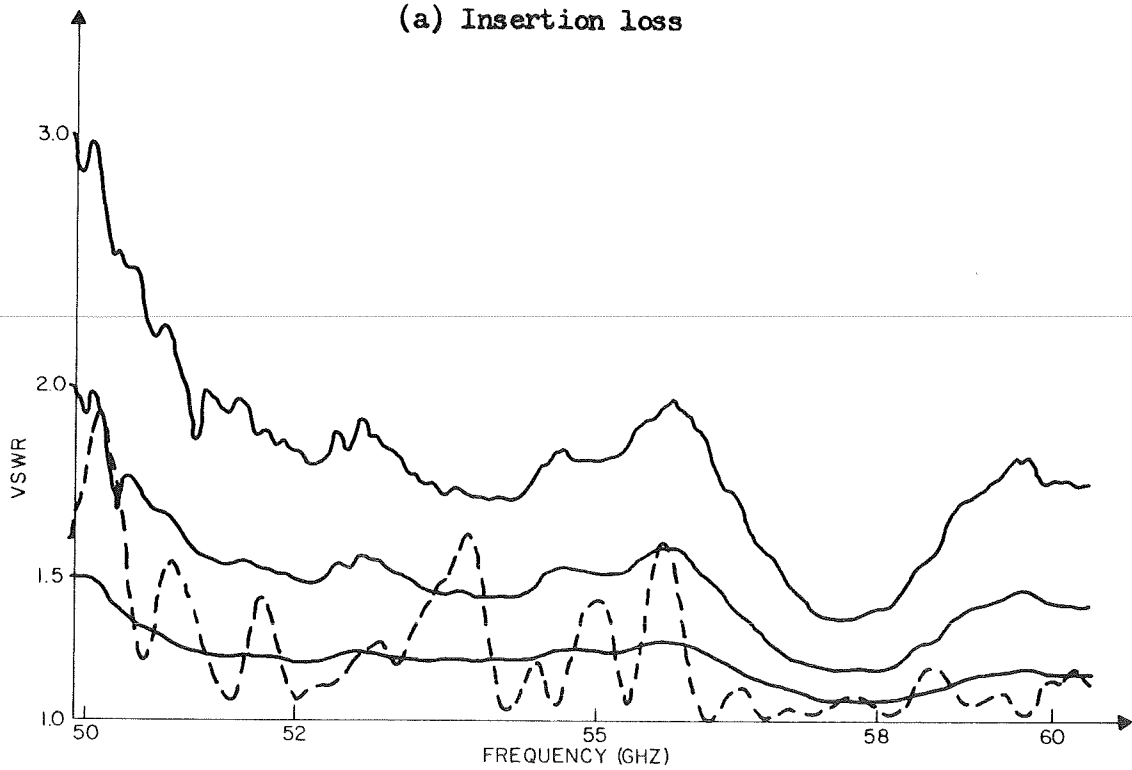


Figure 16. Four bit differential phase shift at 20 frequencies. Individual bit data taken only at the five frequencies indicated.



(a) Insertion loss



(b) VSWR

Figure 17. Insertion loss and VSWR curves.



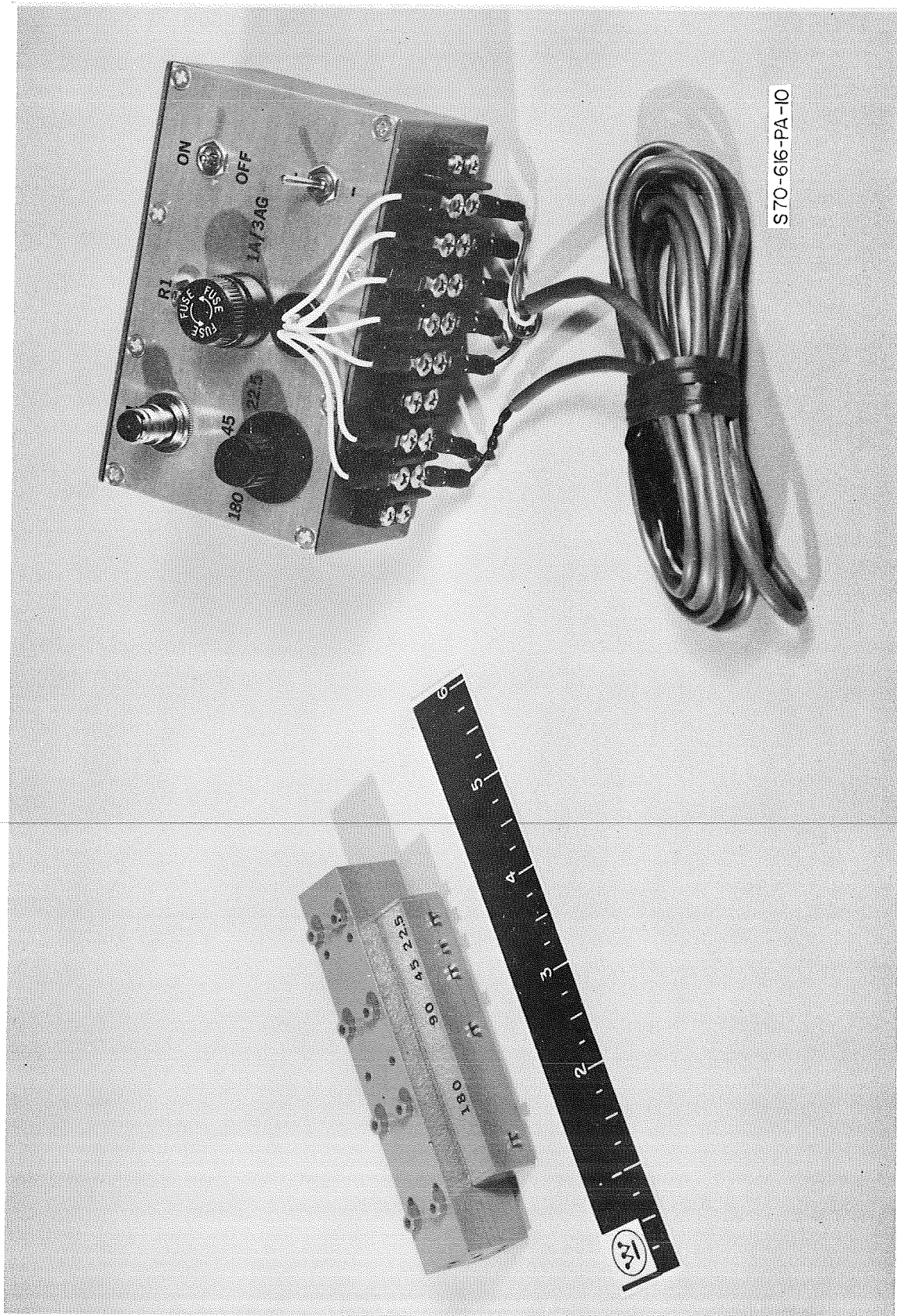
4. OPERATING INSTRUCTIONS

A photograph of the finished phase shifter and driver is shown in figure 18. The driver requires connection to a 12 volt battery or supply capable of delivering a three ampere pulse. Battery connection is made using the two leftmost terminals of the strip visible in the figure. R1 is an output vernier current adjustment and need not be touched. The polarity reversing toggle switch is at the lower right hand corner of the driver. A schematic of the driver is presented in figure 19. Phase shifter to driver connections are shown in figure 20. To operate the device proceed as follows:

1. Connect Driver to 12 V supply or battery capable of delivering 3 amp pulse.
2. Connect Driver to phase shifter as shown in figure 20.
3. Turn Driver on using switch provided.
4. Select bit to be latched using rotary switch.
5. Select polarity of latching pulse using polarity switch.
6. Pressing S1 applies a 3 amp, 14 μ sec. pulse to latch the bit selected.

Note 1: Current from any one of the individual bit latching wire pairs is capable of latching all four bits in series. To do this connect any one of the individual bit wire pairs to the endmost phase shifter terminals and turn the bit selector knob to the corresponding bit position; then proceed as in steps 5 and 6.

Note 2: Reversing the battery polarity by mis-connecting the battery leads may seriously damage the pulser. Red lead goes to battery positive terminal, black lead to negative.



S70-616-PA-10

Figure 18. Finished phase shifter and driver.

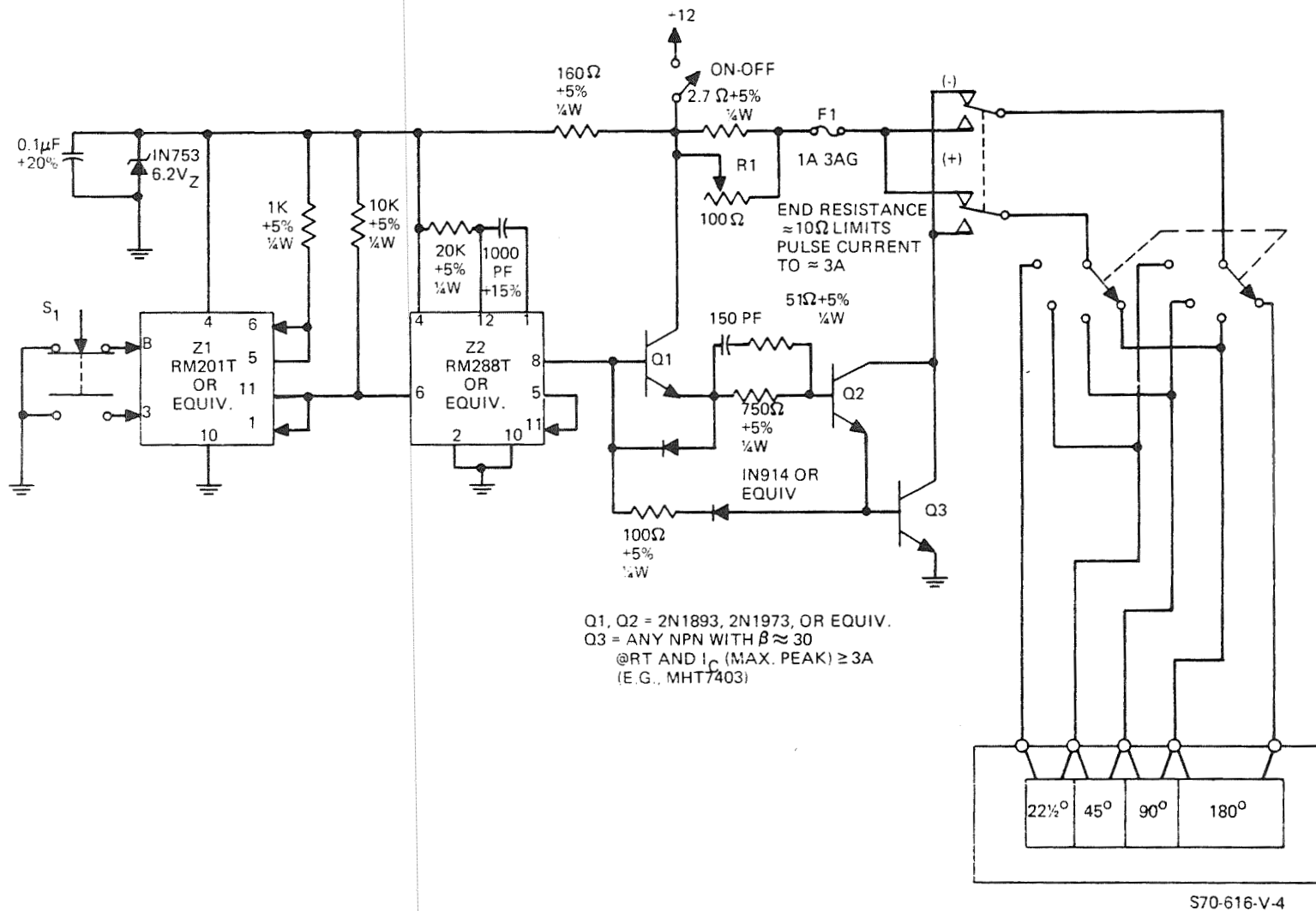
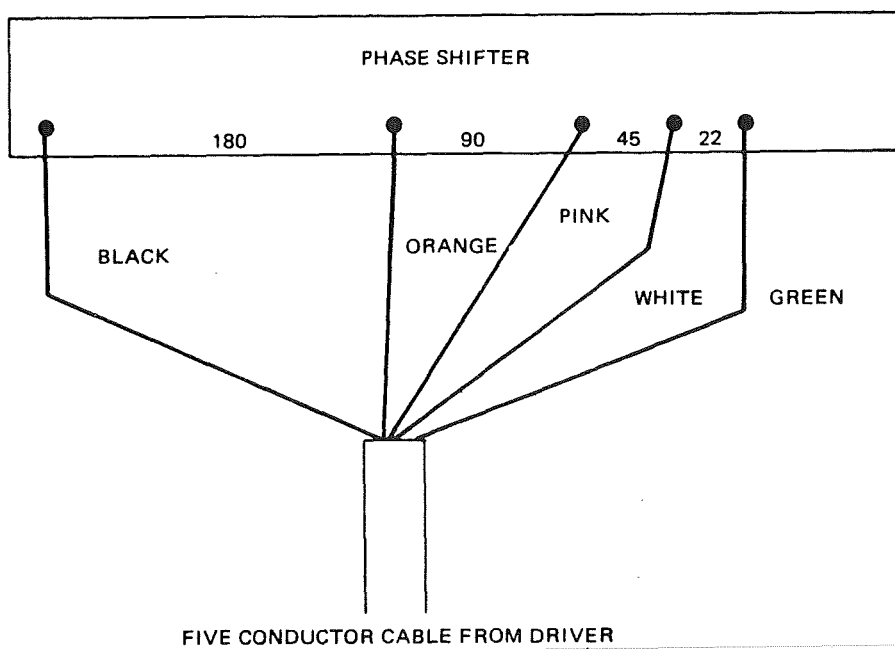


Figure 19. Schematic diagram of current pulser.



S70-616-V-3

Figure 20. Phase shifter-driver interconnection.



5. CONCLUSIONS AND RECOMMENDATIONS

Although the scope of this program was somewhat limited by the available time and funds, several important conclusions can be drawn:

- 1) It is possible to fabricate a 50-60 GHz digital latching phase shifter making the waveguide housing using conventional machining techniques, but only by sacrificing performance.
- 2) In addition, a conventional machining approach is sufficient, at best, for manufacturing very small (one or two-of-kind) quantities of devices. Development and manufacturing problems associated with large quantities would be intolerably expensive and time consuming.
- 3) The loss of the final 4 bit unit was higher than desired averaging 4-5 dB over the bands of interest due to the method of constructing the waveguide housing. However, measurements on 180° bits in a $1\frac{1}{2}$ " test fixture indicate that an insertion loss of 2.0-2.5 dB could be achieved in a 4 bit unit with a low loss housing, preferably electroformed.
- 4) The best approach for fabricating millimeter wave phase shifters would involve electroforming the housing about either a conventional toroid or preferably a twin ferrite slab.
- 5) The technique of using twin ferrite slabs in place of toroids shows much promise but it has yet to be demonstrated that it is possible to complete the magnetic path on the very small slabs with negligible loss of remanent magnetization.

Based on these conclusions and the results of this program, it is recommended that further work be concentrated on developing the electroforming process for fabricating the housing and continuing the investigation of the ferrite twin slab approach for fabricating the phase shifting element.



Another area of investigation that would be of significant benefit to any future program is that of material properties. It is highly recommended that a fundamental investigation of material properties in this frequency range, in particular the loss factors ϵ'' and μ'' , be initiated since all calculations of loss and, in turn, figure of merit (degrees/dB) depend on an exact knowledge of these material properties. During this program (see section 2.3) for example, using 10 GHz values for the ferrite loss tangent in the computer calculations, yielded figures of merit in excess of $300^\circ/\text{dB}$ when experimentally the best that was ever achieved for a 180° bit in a test fixture was $180^\circ/\text{dB}$. Thus for any realistic and meaningful calculation of the maximum figure of merit to be expected in a millimeter wave phase shifter, experimentally measured values of material parameters will be absolutely essential.



6. NEW TECHNOLOGY APPENDIX

After a diligent review of the work performed on this program and a diligent review of this report, we conclude that there are no new technology developments to report.